



Additional diagnostic value of new CT imaging techniques for the functional assessment of coronary artery disease: a meta-analysis

Michèle Hamon^{1,2} · Damien Geindreau^{1,2} · Lydia Guittet^{2,3} · Christophe Bauters^{4,5} · Martial Hamon²

Received: 4 July 2018 / Revised: 30 October 2018 / Accepted: 27 November 2018 / Published online: 7 January 2019
© European Society of Radiology 2019

Abstract

Objectives To determine the diagnostic performance of cardiac computed tomography (CT)-based modalities including coronary CT angiography (CTA), stress myocardial CT perfusion (stress CTP), computer simulation of fractional flow reserve by CT (FFR_{CT}), and transluminal attenuation gradients (TAG), for the diagnosis of hemodynamic significant coronary artery disease (CAD), using invasive fractional flow reserve as the reference standard.

Methods PubMed and Cochrane databases were searched for original articles until July 2018. Diagnostic accuracy results were pooled at per-patient and per-vessel level using random effect models.

Results Fifty articles were included in the meta-analysis (3024 subjects). The per-patient analysis per imaging modality demonstrated a pooled positive likelihood ratio (PLR) of 1.78 (95% confidence interval CI 1.49–2.11), 4.58 (95% CI 3.54–5.91), and 3.45 (95% CI 2.38–5.00) for CTA, stress CTP, and FFR_{CT} respectively. Per-patient specificity of stress CTP (82%, 95% CI 76–86) and FFR_{CT} (72%, 95% CI 68–76) were higher than for CTA (48%, 95% CI 44–51). At the vessel level, PLR was 2.42 (95% CI 1.93–3.02), 7.72 (95% CI 5.50–10.83), 3.50 (95% CI 2.73–4.78), 1.97 (95% CI 1.32–2.93) for CTA, stress CTP, FFR_{CT}, and TAG respectively.

Conclusion With improved PLR and specificity, stress CTP and FFR_{CT} have incremental value over CTA for the detection of functionally significant CAD.

Key Points

- *New functional CT imaging techniques, such as stress CTP and FFR_{CT}, improve diagnostic accuracy of coronary CTA to predict hemodynamically relevant stenosis.*
- *TAG yields poor diagnostic performance.*
- *Combination of CTA and some functional CT techniques (stress CTP and FFR_{CT}) might become a “must” to improve diagnostic accuracy of CAD and to reduce unnecessary invasive coronary angiography.*

Keywords Coronary angiography · Myocardial perfusion imaging · Computed tomography angiography · Myocardial fractional flow reserve · Coronary artery disease

Electronic supplementary material The online version of this article (<https://doi.org/10.1007/s00330-018-5919-8>) contains supplementary material, which is available to authorized users.

✉ Michèle Hamon
michele.hamon@unicaen.fr

¹ Département de Radiologie, Centre Hospitalier Universitaire de Caen, Avenue Côte de Nacre, 14033 Caen, Normandie, France

² Université de Caen, UFR de Médecine, Caen, Normandie, France

³ Département d'Information Médicale, Centre Hospitalier Universitaire de Caen, Caen, Normandie, France

⁴ Département de Cardiologie, Centre Hospitalier Universitaire Régional de Lille, Lille, Hauts de France, France

⁵ INSERM U1167, Université de Lille, UFR de Médecine, Lille, Hauts de France, France

Abbreviations

AUC	Area under the curve
CABG	Coronary artery bypass grafting
CAD	Coronary artery disease
CT	Computed tomography
CTA	Coronary computed tomography angiography
CTP	Computed tomography perfusion
FFR _{CT}	Computer simulation of fractional flow reserve based on computed tomography
FN	False negative
FP	False positive
HU	Hounsfield units
iFFR	Invasive fractional flow reserve
mSv	milliSievert
NLR	Negative likelihood ratio
NPV	Negative predictive value

PLR	Positive likelihood ratio
PPV	Positive predictive value
TAG	Transluminal attenuation gradient
TN	True negative
TP	True positive

Introduction

Given its high negative predictive value (NPV), coronary computed tomography angiography (CTA) of coronary arteries is routinely recommended to rule out obstructive coronary artery disease (CAD) in patients with low and intermediate risk of CAD [1, 2]. Recently, novel computed tomography (CT) imaging techniques, such as stress myocardial computed tomography perfusion (stress CTP), fractional flow reserve calculated by CT (FFR_{CT}), and transluminal attenuation gradient (TAG), have emerged as potential strategies able to combine both anatomical and functional evaluation with potential positive impact on the diagnosis performance [3]. CTP evaluates myocardial perfusion by analyzing the iodine uptake of myocardium during the first pass of contrast. FFR_{CT} is obtained by the application of computational fluid dynamics principles to standard coronary CTA data set, allowing non-invasive assessment of FFR. TAG gives contrast-based flow estimations by analyzing the differences in contrast densities proximal and distal to a stenosis; TAG is defined as the linear regression coefficient between luminal contrast attenuation in Hounsfield units (HU) and length from the ostium.

In terms of functional assessment, the invasive fractional flow reserve measurement during coronary angiography (iFFR) is considered the reference standard for detection of significant coronary lesions. The clinical value of iFFR to guide revascularization therapy has been well established by several prospective randomized trials [4–6]. Whether or not these new CT techniques (stress CTP, FFR_{CT} , and TAG) might improve the diagnostic performance of CTA for the diagnosis of functionally significant CAD using iFFR as the reference standard was the purpose of the present meta-analysis.

Materials and methods

Methods

The meta-analysis was performed according to standard guidelines from the Preferred Reporting Items for Systematic Reviews and Meta-analyses [7].

Search strategy

Database search for articles published in English up to July 2018, using CTA, stress CTP, FFR_{CT} , and TAG as CT

diagnostic techniques, was performed in MEDLINE, and Cochrane databases, by two investigators independently (MH, DG). We used the following search with Medical Subject Headings (MeSH) and non-MESH search terms: coronary angiography (MeSH Terms), myocardial fractional flow reserve (MeSH Terms), computed tomography (MeSH Terms), myocardial perfusion imaging (MeSH Terms), and transluminal attenuation gradient. We also scanned references in retrieved articles and reviews.

The retrieved studies were carefully examined by the same two investigators (MH, DG) to exclude potentially duplicate or overlapping data. Meetings abstracts were excluded, as they could not provide adequately detailed data and their results might not be final. Only papers evaluating the presence of hemodynamically significant CAD by both iFFR and CT technique in the same patients were included. Disagreements were resolved by consensus by the same two authors.

Study selection

We included a study if (i) it used CTA, stress CTP, FFR_{CT} , and/or TAG as diagnostic test to detect hemodynamically relevant CAD; (ii) reported cases in absolute numbers of true-positive (TP), false-positive (FP), true-negative (TN), and false-negative (FN) results or presented sufficiently detailed data for deriving these figures; and (iii) used iFFR as the reference standard. Studies evaluating only rest CT perfusion without stress were excluded from the analysis. Only the papers concerning patients with stable chest pain were included.

Data extraction and quality assessment

The same two investigators (MH, DG) performed the data extraction independently, and discrepancies were resolved by consensus. The following information was extracted from each study: first author, journal and year of publication, study design, study population characteristics including inclusion and exclusion criteria, sample size (number of lesions and subjects evaluated with both tests without minimal sample size), mean age, percentage male, technical characteristics of the CT, including type and brand of machine used, technical parameters for CT acquisition: radiation dose (mSv), amount of iodine contrast (g), imaging protocol including for stress CTP (z -axis coverage, stressor, static versus dynamic acquisition), analysis protocol including assessment criteria for CTA, stress CTP, FFR_{CT} , TAG, FFR_{CT} software, and iFFR criteria and threshold. In cases where > 1 diagnostic CT technique was evaluated within a single publication, each modality was considered separately except for stress CTP, which was evaluated in combination with CTA results.

The study quality conformed to the QUADAS 2 [8].

Data synthesis and statistical analysis

For CTA analysis, a positive test was defined as $\geq 50\%$ coronary artery stenosis.

Categorical variables from individual studies are presented as n/N (%) and continuous variables are presented as median values. Measures of diagnostic accuracy are reported as point estimates (with 95% CI).

By means of TP, TN, FP, and FN rates, we computed sensitivity, specificity, positive and negative predictive values (PPV and NPV), positive and negative likelihood ratios (PLR and NLR), and diagnostic odds ratios. Diagnostic performance analysis was conducted both at the per-patient and per-vessel levels.

We computed all statistics for individual studies and then combined them using a random-effects model, weighting each point estimate by the inverse of the sum of its variance and the between-study variance. Between-study statistical heterogeneity was assessed using the Cochran Q chi-square and I-square tests. Potential publication bias per modalities was assessed by creating funnel plots.

Fagan's nomogram analysis was conducted to evaluate a patient's probability of having or not a significant functional CAD after the index test result.

Statistical computations were performed with Meta-DiSc 1.4 [9].

Results

The reviewing process is described in Fig. 1 (flow chart). We finally included 50 studies (3024 subjects), in this systematic review [10–59].

Characteristics of studies

All studies were published between 2008 and 2018. Design study, index test, inclusion and exclusion criteria, and reference test characteristics including pre-selection criteria for iFFR evaluation are reported in Table 1.

Population characteristics and imaging protocols for studies evaluating CTA (Table 1), stress CTP (Tables 1 and 2), FFR_{CT} (Tables 1 and 3), and TAG (Table 1) are listed. The entire group of studies included subjects with a mean age of 57 [11, 43, 55] to 73 [49] years old, and the proportion of males ranged from 32% [45] to 100% [11]. Studies were performed with 64-slice to 320-slice CT. Thirty studies reported effective radiation dose. The range of effective radiation dose was 1–9 millisieverts (mSv) for CTA alone, 3–16 mSv for the total combined CTA and stress CTP, 0.7–15 mSv for FFR_{CT}, and 3–15 mSv for TAG.

The amount of iodine contrast, available in 26 studies, ranged from 17 to 56 g.

All stress CTP studies used adenosine as stressor agent at a dose of 140 $\mu\text{g}/\text{kg}/\text{min}$; all stress CTP studies were performed

using single-energy mode. Z coverage ranged from 38 to 160 mm [20–35]. Static first pass acquisition was used in nine studies [21–24, 28, 30, 32, 33, 35], while seven studies used dynamic acquisition (six in shuttle mode [20, 25, 27, 29, 31, 34] and one in stationary mode [26]). In one study [26], only stress CTP without CTA was performed; in another one [24], only one acquisition for both CTA and stress CTP analysis was performed; for all the other studies, two acquisitions were performed (one at rest used for CTA analysis and one at stress for myocardial perfusion analysis) [20–23, 25, 27–35] (Table 2).

For FFR_{CT} analysis, off-site analysis (Heart Flow) was performed in six studies [36–39, 46, 49], while on-site software was used in 12 studies [30, 31, 40–45, 47, 48, 50, 51]. All studies used ≤ 0.80 as FFR_{CT} threshold for hemodynamically significant CAD (Table 3).

For TAG studies, different cutoffs were used, ranging from -0.645 to -1.537 UH/mm [42, 52, 53, 55–57]. Three studies were exclusively performed with large 320-slice CT [54, 58, 59].

Quality assessment

The overall quality of the studies according to the QUADAS 2 tool was high. Study quality assessment is reported in Fig. 2.

Pooled diagnostic accuracy

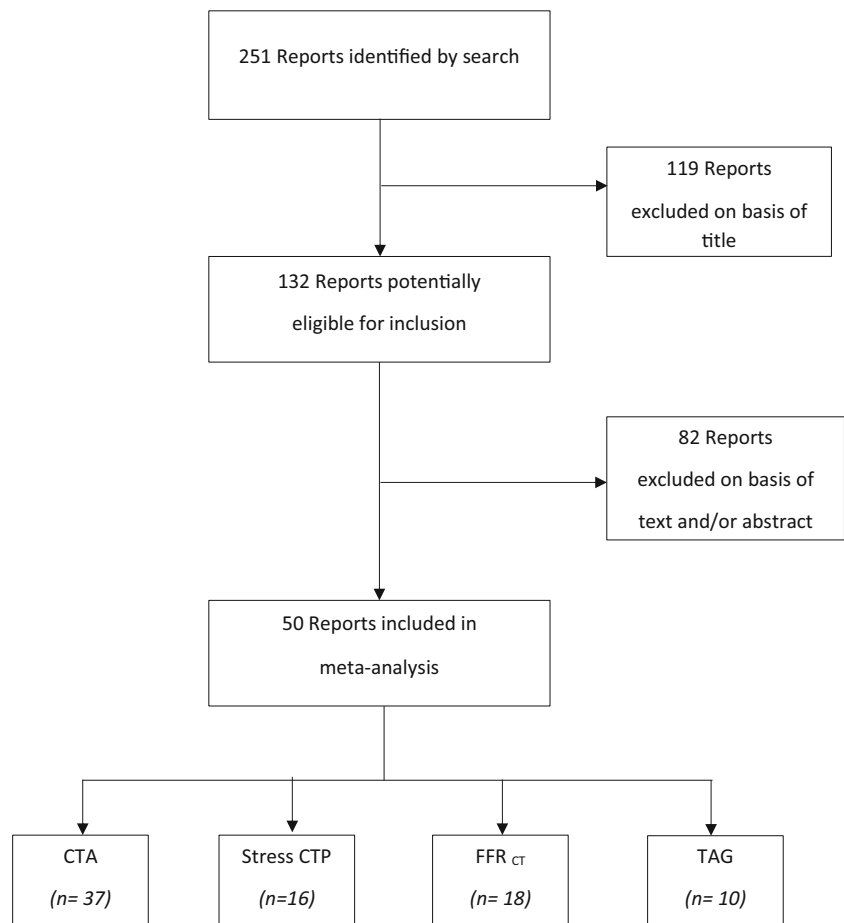
For the results, the articles included in the meta-analysis were divided into four groups based on CT-modality evaluated (CTA, stress CTP, FFR_{CT}, and TAG). TAG was only available at vessel level analysis. Overall diagnostic accuracy at the patient level and the vessel level are reported in Table 4 and in Forest plots (Figs. 3 and 4).

The per-patient analysis demonstrated a pooled PLR of 1.78, 4.58, and 3.45 for CTA, stress CTP, and FFR_{CT} respectively. At the vessel level, PLR were 2.42, 7.72, 3.50, and 1.97 for CTA, stress CTP, FFR_{CT}, and TAG respectively.

Given the different PLR of CTA, stress CTP, FFR_{CT}, and TAG, if we use the Fagan's nomogram (Fig. 5): for a pre-test probability of 30%, the post-test probability of hemodynamically significant CAD would raise to 43% for CTA, 65% for stress CTP and 60% for FFR_{CT} on a per-patient analysis and to 51% for CTA, 77% for stress CTP, 60% for FFR_{CT} and 46% for TAG on a per vessel-analysis. For NLR, there is no difference between CTA, stress CTP, and FFR_{CT}, respectively, 0.21, 0.21, and 0.23 at vessel level. Hence, with a pre-test probability of 30% on a per-vessel basis, the post-test probability given a negative test would lower to 8%, 4%, and 7% for CTA, stress CTP, and FFR_{CT} respectively. With a NLR of 0.67 for TAG, the post-test probability would only lower to 22%.

For stress CTP and FFR_{CT}, the summary receiver operating characteristic curve demonstrated superior diagnostic accuracy when compared with CTA alone or TAG (Table 4). This finding was observed at both patient and vessel level.

Fig. 1 Flowchart describing the publication search and selection of eligible studies. Abbreviations: *n* = number of studies



Separate analyses have been performed at vessel level for the different CT modalities owing to various technical approaches (Table 5). For stress CTP, sub-analysis demonstrated better PLR for static than for dynamic mode, with PLR of 10.77 and 4.89, respectively. For FFR_{CT}, separate analysis of off-site compared to on-site post-processing demonstrated similar performance with PLR of 3.05 and 3.67, respectively. Overall performance of TAG is poor; however, sub-analysis showed higher diagnostic performance for > 320-slice CT than for < 320-slice CT, with PLR of 3.53 and 0.61 respectively.

On a per-patient basis, statistical heterogeneity was observed for CTA (for sensitivity, specificity, PLR, PPV, and NPV), for stress CTP (for NPV), and for FFR_{CT} (for specificity and PLR). At lesion level, heterogeneity exists for all modalities except for FFR_{CT} (for sensitivity, PPV and NLR) and for TAG (for NPV), justifying the use of the random effect model.

Funnel plots per modalities at patient and vessel level are shown on eFig.1 and eFig.2 (electronic supplementary material).

Discussion

In the present analysis, stress CTP and FFR_{CT}, which provide additional functional information, demonstrated improved

diagnostic PLR and specificity compared with stand-alone CTA for the detection of hemodynamically relevant stenosis, both at the patient and vessel level. Conversely, TAG (with an area under the curve (AUC) of 0.65) demonstrates poor diagnostic accuracy for the diagnosis of hemodynamically relevant stenosis.

CTA is a non-invasive technique providing only anatomic CAD information. As already known, CTA has a high NPV and low NLR and is recommended as a test for ruling out significant obstructive CAD in symptomatic patients with low to intermediate likelihood of CAD [2]. However, mainly due to the presence of artifacts related to coronary calcification, the PLR and specificity of CTA is not sufficiently high, resulting in false-positive studies or inconclusive studies leading to potential unnecessary referral to invasive coronary angiography or to further functional diagnostic tests (stress MRI, stress echo, or stress SPECT).

In our meta-analysis, CTA alone yields only relatively low PLR (1.8 on per patient and 2.4 on per-vessel analysis) and very low specificity (48% on per patient, 64% on per-vessel analysis) for the diagnosis of hemodynamically significant CAD.

Stress CTP and FFR_{CT} offer higher PLR (4.6 and 3.4 on a per-patient analysis, and 7.7 and 3.5 on a per-vessel analysis respectively) and higher specificity (82% and 72% on a per-patient analysis, 89% and 75% on a per-vessel analysis respectively).

Table 1 Summary characteristics of included studies

Author, journal, year	Design	Index test	Study population Inclusion	Study population Exclusion	Patient N (%male)	Mean age \pm SD (N)	Lesion	Hardware	Radiation dose (mSv)	Iodine (g)	ICA criteria for iFFR	iFFR threshold
Meijboom et al [10] JACC, 2008	S Retrospective	CTA	Known CAD	Stent, CABG	79 (81)	60 \pm 9	89	64-slice CT Sensation or 128-slice DSCT Definition FLASH Siemens Healthcare	NA	22–40	Interventional cardiologist discretion	< 0.75, < 0.8*
van Werkhoven et al [11] Am J Cardiol, 2009	S Retrospective	CTA	Suspected or known CAD	–	33 (100)	57 \pm 11	36	64-row CT Aquilion 64	NA	NA	–	\leq 0.75
Sarno et al [12] JACC Img, 2009	S Prospective	CTA	Suspected or known CAD	–	81 (74)	62 \pm 11	116	Toshiba Medical Systems 64-slice CT Sensation Siemens Healthcare	NA	36	–	\leq 0.75
Kristensen et al [13] Int J Cardiol, 2010	S Prospective	CTA	Intermediate lesion on diagnostic ICA	–	42 (90)	61 \pm 10	56	64-row CT Aquilion 64	NA	NA	Intermediate stenosis on ICA	< 0.75
Oposlki et al [14] Eur J Radiol, 2014	S Prospective	CTA	50–80% stenosis on CTA	Stent, CABG, prior MI, LM, heavily calcified lesions	61 (64)	63 \pm 9	71	Toshiba Medical Systems 64-slice DSCT Somatom Definition Siemens Healthcare	NA	32–48	\geq 50–80% stenosis on CTA	\leq 0.8
Rossi A et al [15] Circ Cv Img, 2014	M (2) Retrospective	CTA	Known CAD	LM, heavily calcified lesions	99 (78)	61 \pm 11	144	64-slice DSCT Somatom Definition 128-slice DSCT Definition FLASH Siemens Healthcare	NA	18–37	Interventional cardiologist discretion	\leq 0.8
Voros et al [16] Am J Cardiol, 2014	S Prospective	CTA	Suspected or known CAD	–	85 (62)	61 \pm 8	85	64-slice Somatom Siemens Healthcare 320-row CT Aquilion One Toshiba Medical Systems	NA	NA	40–99% stenosis on CTA or ICA	\leq 0.75
Ko et al [17] Eur Radiol, 2014	S Retrospective	CTA	Suspected CAD	CABG, recent MI	115 (76)	64 \pm 10	230	320-row CT Aquilion One	4.5 \pm 3.1	NA	Interventional cardiologist discretion	\leq 0.8
Guektere et al [18] Int J Cv Img 2015	S Prospective	CTA	Suspected or known CAD	–	65 (72)	63 \pm 9	52	Toshiba Medical Systems 64 LightSpeed or Discovery CT 750 HD	NA	28–36	40–70% stenosis on ICA	\leq 0.8
Danad et al [19] JAMA Cardiol, 2017	S Prospective	CTA	Suspected CAD	Acute MI	208 (65)	58 \pm 9	615	GE Healthcare 256-section CT Brilliance iCT	5.31 \pm 1.32	NA	All coronary arteries	\leq 0.8
Bamberg et al [20] Radiology, 2011	S Prospective	CTA Stress CTP	Suspected or known CAD	–	33 (76)	68 \pm 10	96	128-slice DSCT Definition FLASH Siemens Healthcare	3.1 \pm 1 CTA 10 \pm 2 sCTP	NA	50–85% stenosis on ICA	\leq 0.75
Ko et al [21] Eur Heart J, 2012	S Prospective	CTA Stress CTP	Known CAD (at least one > 50% stenosis by ICA) referred for non urgent revascularization by PCA	CABG, Recent MI LM, CTO	42 (64)	65 \pm 8	86	320-row CT Aquilion One Toshiba Medical Systems	5.3 \pm 2.2 sCTP 4.8 \pm 2.6 CTA	42	\geq 50% stenosis on ICA	\leq 0.8
Ko et al [22] JACC Img, 2012	S Prospective	CTA Stress CTP	Suspected CAD	Known CAD Recent ACS	28 (67)	62 \pm 10	103	320-row CT Aquilion One	4.7 \pm 3.9 CTA 4.5 \pm 1.9 sCTP	42	All major vessels	\leq 0.8
Beitencourt et al [23] JACC, 2013	S Prospective	CTA Stress CTP	Suspected CAD	–	101 (67)	62 \pm 8	303	64-slice CT Sensation Siemens Healthcare	Total 5 \pm 0.96	NA	> 40% stenosis on ICA	\leq 0.8

Table 1 (continued)

Author, journal, year	Design	Index test	Study population Inclusion	Study population Exclusion	Patient N (%male)	Mean age ± SD (N)	Lesion	Hardware	Radiation dose (mSv)	Iodine (g)	ICA criteria for iFFR	iFFR threshold
Choo et al [24] <i>Acta Radiol</i> , 2013	S Prospective	CTA Stress CTP	Suspected CAD (symptomatic at low to intermediate risk of CAD) and > 50% diameter stenosis on CTA	Stent, CABG, prior MI	37 (75)	62 ± 20	81	128-slice DSCT Definition FLASH Siemens Healthcare	4.63 ± 2.57	27	50–85% stenosis on ICA	≤ 0.75
Greif et al [25] <i>Heart</i> , 2013	S Prospective	CTA Stress CTP	Suspected or known CA, including stent, or CABG	–	65 (64)	70 ± 9	195	128-slice DSCT Definition FLASH Siemens Healthcare	2.9 ± 0.9 CTA 9.7 ± 2.2 sCTP	NA	50–85% stenosis on ICA	≤ 0.8
Huber et al [26] <i>Radiology</i> , 2013	S Prospective	Stress CTP	Suspected CAD	Recent ACS	32 (66)	63 ± 8	96	256-section CT Brilliance iCT Philips Healthcare	9.5	16	–	< 0.75
Rossi et al [27] <i>Eur Heart J Cv Img</i> , 2014	M(2) Prospective	CTA Stress CTP	Suspected CAD	–	80 (79)	60 ± 10	210	128-slice DSCT Definition FLASH Siemens Healthcare	4.2 CTA 9.4 sCTP	21–50	30–90% stenosis on ICA	≤ 0.75
Wong et al [28] <i>JACC</i> , 2014	S Prospective	CTA + Stress CTP	Suspected or known CAD	CABG, recent MI	75 (69)	64 ± 11	123	Siemens Healthcare 320-row CT Aquilion One Toshiba Medical Systems	4.6 ± 3.2 CTA 4.8 ± 3.5 sCTP	42	≥ 30% stenosis on ICA	≤ 0.8
Kono et al [29] <i>Investigative Radiol</i> , 2014	S Prospective	CTA + Stress CTP	Suspected or known CAD	Prior MI	42 (81)	62 ± 19	91	128-slice DSCT Definition FLASH Siemens Healthcare	3.5 CTA 9.4 sCTP	33–37	–	≤ 0.8
Yang et al [30] <i>Radiology</i> , 2015	S Prospective	CTA Stress CTP	Suspected or known CAD (symptomatic at intermediate to high risk of CAD)	CABG, prior PCI	75 (77)	64 ± 10	210	Siemens Healthcare 128-slice DSCT Definition FLASH Siemens Healthcare	NA	48–56	–	≤ 0.8
Coenen, et al [31] <i>JACC Img</i> , 2017	M(2) Prospective	CTA Stress CTP	Suspected or known CAD	CTO	74 (84)	61 ± 9	142	128-slice DSCT Definition FLASH Siemens Healthcare	3.7 ± 3.2 CTA 9.3 ± 0.18 sCTP	NA	30–90% stenosis on ICA	≤ 0.8
Yang et al [32] <i>Eur Heart J Cv Img</i> , 2017	S Prospective	CTA Stress CTP	Suspected CAD	CABG, PCI, CTO	72 (89)	63 ± 9	168	128-slice DSCT Definition FLASH Siemens Healthcare	7.8 ± 2.8 CTA 7.7 ± 3.0 sCTP	NA	20–90% stenosis on ICA	≤ 0.8
Williams et al [33] <i>Eur Radiol</i> , 2017	S Prospective	Stress CTP	Suspected or known CAD referred for clinically indicated ICA	–	51 (80)	63 ± 2	141	Siemens Healthcare 320-row CT Aquilion One	2.73 CTA 3.71 sCTP	NA	≥ 50% stenosis on ICA	≤ 0.8
Coenen et al [34] <i>Eur Radiol</i> , 2017	S Prospective	Stress CTP	Suspected CAD referred for indicated invasive angiography	–	43 (84)	63 ± 9	94	Toshiba Medical Systems 128-slice DSCT Definition FLASH Siemens Healthcare	9.0 ± 0.19 sCTP	18	30–90% stenosis on ICA	≤ 0.8
Pontone et al [35] <i>JACC Img</i> , 2018	S Prospective	CTA Stress CTP	Suspected CAD	Prior MI, Prior PCI CABG, ACS	100 (69)	66 ± 9	–	256-Slice CT Revolution GE Healthcare	2.8 ± 1.4 CTA 2.5 ± 1.1 sCTP	22	30–80% stenosis on ICA	≤ 0.8
Koo et al [36] <i>JACC</i> , 2011	M(4) Prospective	CTA FFR _{CT}	Suspected or known CAD referred for clinically indicated ICA, with CTA ≥ 50% stenosis	CABG	103 (72)	63 ± 8	159	≥ 64 slices multivendor	3–15	26–37	Clinically indicated	≤ 0.8
Min, et al [37] <i>JAMA</i> , 2012	M(17) Prospective	CTA FFR _{CT}	Suspected or known CAD referred for clinically indicated non urgent ICA	CABG, Prior PCI	252 (71)	63 ± 9	407	≥ 64 slices multivendor	4.4–15	NA	30–90% stenosis on ICA	≤ 0.8

Table 1 (continued)

Author, journal, year	Design	Index test	Study population Inclusion	Study population Exclusion	Patient N (%male)	Mean age \pm SD (N)	Lesion	Hardware	Radiation dose (mSv)	Iodine (g)	ICA criteria for iFFR	iFFR threshold
Norgaard et al [38] <i>JACC</i> , 2014	M (10) Prospective	CTA FFR _{CT}	Suspected CAD referred for clinically indicated non urgent ICA, with CTA 30–90% stenosis	CABG, PCI ACS	254 (64)	64 \pm 10	484	≥ 64 slices Multivendor	3.0 \pm 2.2 Pro 14.3 \pm 7.0 Retro	NA	$\geq 30\%$ stenosis on ICA	≤ 0.8
Kim et al [39] <i>JACC Img</i> , 2014	M (3) Prospective	CTA FFR _{CT}	Suspected or known CAD referred for clinically indicated non urgent ICA with CTA $\geq 50\%$ stenosis	–	44 (80)	65 \pm 9	48	≥ 64 slices Multivendor	NA	NA	Interventional cardiologist discretion	≤ 0.8
Renker et al [40] <i>Am J Cardiol</i> , 2014	S Retrospective	FFR _{CT}	Suspected or known CAD	Stent, CABG, Bifurcation lesion	53 (64)	61 \pm 12	67	64-slice DSCT Definition 128-slice DSCT Definition FLASH Siemens Healthcare	NA	NA	Interventional cardiologist discretion	≤ 0.8
Coenen et al [41] <i>Radiology</i> , 2015	S Retrospective	CTA FFR _{CT}	Suspected or known	CABG, PCI, CA score > 2000	106 (77)	61 \pm 9	189	64-slice DSCT Definition 128-slice DSCT Definition FLASH Siemens Healthcare	7.6	NA	Interventional cardiologist discretion	≤ 0.8
Wang et al [42] <i>Eur J Radiol</i> , 2015	S Retrospective	CTA FFR _{CT} , TAG	Suspected CAD	Stent, CABG, LM, CTO, Bifurcation	32 (66)	58 \pm 12	32	64-slice DSCT Definition 128-slice DSCT Definition FLASH Siemens Healthcare	7.7 \pm 1	18–44	–	≤ 0.8
Zhang et al [43] <i>PLoS one</i> , 2016	S Retrospective	CTA FFR _{CT}	Suspected CAD	CABG, PCI CA score > 2000	21 (76)	57 \pm 10	32	64-slice Aquilion 320-row CT Aquilion One Toshiba Medical Systems	NA	NA	Interventional cardiologist discretion	≤ 0.8
De Geer et al [44] <i>Acta Radiol</i> , 2016	S Retrospective	FFR _{CT}	Suspected CAD	CABG, PCI, ostial stenosis	21 (52)	60 \pm 9	23	128-slice DSCT Definition FLASH Siemens Healthcare	0.7–14.1	NA	–	≤ 0.75 $\leq 0.8^{**}$
Kruk et al [45] <i>JACC Img</i> , 2016	S Prospective	CTA FFR _{CT}	Suspected CAD referred for clinically indicated non urgent ICA, with CTA 50–90% stenosis	CABG, prior MI, CTO	90 (32)	63.4 \pm 8.2	96	Siemens Healthcare 128-slice DSCT Definition FLASH Siemens Healthcare	7.3	24–32	Interventional cardiologist discretion	≤ 0.8
Kawaji et al [46] <i>Int J Cv Img</i> , 2016	M (2) Prospective	FFR _{CT}	Suspected CAD	CABG, PCI, recent prior MI	48 (65)	70.8 \pm 7.8	70	64-slice DSCT Definition, Siemens Healthcare 320-row CT Aquilion One Toshiba Medical Systems	NA	NA	Significant stenosis on CTA or $\geq 30\%$ on ICA	≤ 0.8
Tesche et al [47] <i>JCCT</i> , 2016	S Retrospective	FFR _{CT} TAG	Suspected or known CAD	CABG, PCI, Bifurcation	37 (68)	61 \pm 10	37	64-slice DSCT Definition 128-slice DSCT Definition FLASH Siemens Healthcare	6.6 \pm 0.8	18–30	Intermediate stenosis on ICA	≤ 0.8
Kurata et al [48] <i>Eur Radiol</i> , 2017	S Retrospective	FFR _{CT}	Suspected or known CAD	CABG, PCI, prior MI, CTO	21 (76)	70 \pm 9	29	128-slice DSCT Definition FLASH Siemens Healthcare	8.7 \pm 3.5	17–22	Clinically indicated	≤ 0.8
Osawa et al [49] <i>Heart Vessels</i> , 2017	S Prospective	FFR _{CT}	Suspected CAD and CTA > 30% stenosis	CABG PCI, recent prior MI, ACS	20 (80)	73 \pm 8	26	Siemens Healthcare 128-slice DSCT Definition FLASH Siemens Healthcare	NA	NA	–	≤ 0.8
Shi et al [50] <i>Biomed En Online</i> , 2017	S Retrospective	FFR _{CT}	Suspected CAD with Clinically indicated ICA	–	29 (55)	68 \pm 8	36	320-row CT Aquilion One Toshiba	NA	NA	Clinically indicated	≤ 0.8
Ko et al [51] <i>JACC Img</i> , 2017	S Prospective	CTA FFR _{CT}	Symptomatic at intermediate to high risk of CAD, Clinically indicated ICA with FFR	–	30 (70)	60 \pm 8.5	58	320-row CT Aquilion One Toshiba Medical Systems	4.7	NA	Interventional cardiologist discretion	≤ 0.8

Table 1 (continued)

Author, journal, year	Design	Index test	Study population Inclusion	Study population Exclusion	Patient N (%male)	Mean age \pm SD (N)	Lesion (N)	Hardware	Radiation dose (mSv)	Iodine (g)	ICA criteria for iFFR	iFFR threshold
Yonn et al [52] <i>JACC Img, 2012</i>	S Retrospective	CTA TAG	Suspected or known CAD referred for clinically indicated ICA, with CTA \geq 50% stenosis	CABG	53 (74)	63 \pm 9	82	64-slice Definition Siemens 64 Brilliance, Philips	3–15	32	Clinically indicated	\leq 0.8
Choi et al [53] <i>Eur Heart J, 2012</i>	S Retrospective	CTA TAG	Suspected or known CAD and CTA \geq 50% stenosis and subsequently underwent ICA with iFFR	–	63 (70)	63 \pm 8	97	64-slice Definition Siemens 64 Brilliance, Philips	NA	32	Clinically indicated	\leq 0.8
Wong et al [54] <i>JACC, 2013</i>	S Retrospective	CTA TAG	Clinically indicated ICA with iFFR	CABG, recent MI CTO	54 (65)	63 \pm 9	78	320-row CT Aquilion One Toshiba Medical Systems	5.7 \pm 5.2	NA	–	\leq 0.8
Stuijzand et al [55] <i>JACC Img, 2014</i>	S Prospective	CTA TAG	Intermediate probability of CAD	CABG, PCI Previous MI	85 (60)	57 \pm 10	59	256-section CT Brilliance iCT Philips	4.97 \pm 0.89	35	All territory except occluded or subtotal lesion	\leq 0.8
Hell et al [56] <i>Eur J Radiol, 2015</i>	S Retrospective	TAG	Clinically indicated ICA with iFFR and CTA \geq 50% stenosis	–	59 (75)	64 \pm 11	72	128-slice DSCT Definition FLASH Siemens Healthcare \geq 64 slice	5.0 \pm 5.6	24–28	Clinically indicated	\leq 0.8
Nakanishi et al [57] <i>Int J Cv Img, 2015</i>	M (–) Prospective	TAG	Suspected or known CAD	CABG, PCI, CTO	103 (68)	62 \pm 7	146	Siemens Healthcare \geq 64 slice	NA	NA	Clinically indicated	\leq 0.8
Ko et al [58] <i>Radiology, 2016</i>	M(3) Prospective	TAG	Suspected CAD referred for clinically indicated non urgent ICA and CTA 30–90% stenosis	CABG, PCI ACS	51 (74)	62 \pm 10	82	320-row CT Aquilion One or Toshiba Medical Systems	12.70 \pm 4.8 Retro 3.3 \pm 3.8 Pro	20–26	\geq 30% stenosis ICA	\leq 0.8
Ko et al [59] <i>Int J Cv Img, 2016</i>	S Prospective	CTA TAG	Clinically indicated ICA with iFFR	CABG ACS	27 (70)	65 \pm 10	51	320-row CT Aquilion One Toshiba Medical Systems	3.2 \pm 1.9	20–26	Interventional cardiologist discretion	\leq 0.8

S, single center study; M, multicenter study; MI, myocardial infarction; LM, left main; Ca, calcium; CTO, chronic total occlusion; ACS, acute coronary syndrome; PCI, percutaneous coronary intervention; CABG, coronary artery bypass grafting; DSCT, dual source computed tomography; NA, not available; sCT, stress CTP; Pro, prospective acquisition; Retro, retrospective acquisition

*iFFR threshold used in the meta-analysis

Table 2 Summary characteristics of studies evaluating stress CTP versus iFFR

Author, journal, year	Hardware	CT imaging protocol	Perfusion stressor	Perfusion Z coverage	Perfusion acquisition mode	Perfusion image analysis
Bamberg et al [20] <i>Radiology, 2011</i>	128-slice DSCT <i>Definition FLASH</i> <i>Siemens Healthcare</i>	1. CTA 2. Stress CTP	Adenosine	73 mm	Dynamic (shuttle) Single energy	Quantitative (MBF < 75 mL/100 mL/min)
Ko et al [21] <i>Eur Heart J, 2012</i>	320-row CT <i>Aquilion One</i> <i>Toshiba Medical Systems</i>	1. Stress CTP 2. CT-DE 3. CTA	Adenosine	160 mm	Static first-pass Single energy	Visual
Ko et al [22] <i>JACC Img, 2012</i>	320-row CT <i>Aquilion One</i> <i>Toshiba Medical Systems</i>	1. CTA 2. Stress CTP	Adenosine	160 mm	Static first-pass Single energy	Visual Semi-quantitative
Bettencourt et al [23] <i>JACC, 2013</i>	64-slice CT <i>Sensation</i> <i>Siemens Healthcare</i>	1. Ca scoring 2. Stress CTP 3. CTA	Adenosine	38 mm	Static first-pass Single energy	Visual
Choo et al [24] <i>Acta Radiol, 2013</i>	128-slice DSCT <i>Definition FLASH</i> <i>Siemens Healthcare</i>	Stress (CTP-CTA)	Adenosine	38 mm	Static first-pass Single energy	Visual
Greif et al [25] <i>Heart, 2013</i>	128-slice DSCT <i>Definition FLASH</i> <i>Siemens Healthcare</i>	1. CTA 2. Stress CTP	Adenosine	73 mm	Dynamic (shuttle) Single energy	Quantitative (MBF < 75 mL/100 mL/min)
Huber et al [26] <i>Radiology, 2013</i>	256-section CT <i>Brilliance iCT</i> <i>Philips Healthcare</i>	Stress CTP	Adenosine	78 mm	Dynamic (stationary) Single energy	Semi-quantitative Quantitative (MBF < 75 mL/100 mL/min)
Rossi et al [27] <i>Eur Heart J Cardiovasc Img, 2014</i>	128-slice DSCT <i>Definition FLASH</i> <i>Siemens Healthcare</i>	1. Ca Scoring 2. CTA 3. Stress CTP	Adenosine	73 mm	Dynamic (shuttle) Single energy	Quantitative (MBF < 78 mL/100 mL/min)
Wong et al [28] <i>JACC, 2014</i>	320-row CT <i>Aquilion One</i> <i>Toshiba Medical Systems</i>	1. CTA 2. Stress CTP	Adenosine	160 mm	Static first-pass Single energy	Visual
Kono et al [29] <i>Investigative Radiology, 2014</i>	128-slice DSCT <i>Definition FLASH</i> <i>Siemens Healthcare</i>	1. CTA 2. Stress CTP	Adenosine	73 mm	Dynamic (shuttle) Single energy	Quantitative (MBF ratio)
Yang et al [30] <i>Radiology, 2015</i>	128-slice DSCT <i>Definition FLASH</i> <i>Siemens Healthcare</i>	1. Stress CTP 2. CTA	Adenosine	38 mm	Static first-pass Single energy	Visual
Coenen et al [31] <i>JACC Img, 2017</i>	128-slice <i>Definition FLASH, FORCE</i> <i>Siemens Healthcare</i>	1. CTA 2. Stress CTP	Adenosine	73 mm	Dynamic (shuttle) Single energy	Quantitative (MBF index)
Yang et al [32] <i>Eur heart J Cardiovasc Img, 2017</i>	128-slice DSCT <i>Definition FLASH</i> <i>Siemens Healthcare</i>	1. Stress CTP 2. CTA	Adenosine	38 mm	Static first-pass Single energy	Visual
Williams et al [33] <i>Eur Radiol, 2017</i>	320-row CT <i>Aquilion One</i> <i>Toshiba Medical Systems</i>	1. CTA 2. Stress CTP 3. CT-DE	Adenosine	160 mm	Static first-pass Single energy	Semi-quantitative
Coenen et al [34] <i>Eur Radiol, 2017</i>	128-slice <i>Definition FLASH, FORCE</i> <i>Siemens Healthcare</i>	1. CTA 2. Stress CTP	Adenosine	73 mm	Dynamic (shuttle) Single energy	Semi-quantitative Quantitative (MBF index)
Pontone et al [35] <i>JACC Img, 2018</i>	256-slice CT <i>Revolution</i> <i>GE Healthcare</i>	1. CTA 2. Stress CTP	Adenosine	160 mm	Static first-pass Single energy	Visual

Fagan's nomogram analysis illustrates that in case of a negative result, stress CTP and FFR_{CT} have no incremental value compared to CTA alone to rule out hemodynamically significant CAD. Conversely, in case of a positive test, stress CTP and FFR_{CT} offer incremental value over CTA alone. This suggests that CTA alone can act as an accurate "gate-keeper" in ruling out functionally significant CAD, while stress CTP and FFR_{CT} , with significant reduction in false-positive, can allow better identification of patients with ischemic lesion.

Until now, validation of TAG at rest for the diagnosis of hemodynamically significant CAD has yielded conflicting results [42, 47, 52–59]. Our meta-analysis demonstrates global modest performance of TAG (AUC of 0.61). However, large coverage CT scanners (320-slice CT) are associated with better diagnostic performance with an AUC of 0.83. This could be explained by the ability of these wide coverage CT scanners to perform iso-temporal, single-heartbeat, and whole-heart acquisition. Hence, it seems that the ability of TAG to discriminate between

Table 3 Summary characteristics of studies evaluating FFR_{CT} versus iFFR

Author, journal, year	Index test	Hardware	Image analysis Software FFR _{CT}	FFR _{CT} threshold	Rejected for low image quality
Koo et al [36] <i>JACC, 2011</i>	FFR _{CT}	≥ 64 slices	External laboratory	≤ 0.80	NA
Min et al [37] <i>JAMA, 2012</i>	CTA	<i>multivendor</i>	Heart Flow 1.0		
Nørgaard et al [38] <i>JACC, 2014</i>	FFR _{CT}	≥ 64 slices	External laboratory	≤ 0.80	13%
Kim et al [39] <i>JACC Img, 2014</i>	CTA	<i>Multivendor</i>	Heart Flow 1.2		
Renker et al [40] <i>Am J Cardiol, 2014</i>	FFR _{CT}	≥ 64 slices	External laboratory	≤ 0.80	NA
	CTA	<i>Multivendor</i>	Heart Flow 1.2		
Coenen et al [41] <i>Radiology, 2015</i>	FFR _{CT}	64-slice DSCT Definition	On-site computation	≤ 0.80	5%
	CTA	128-slice DSCT Definition FLASH Siemens Healthcare	Siemens cFFR 1.4		
Wang et al [42] <i>Eur J Radiol, 2015</i>	FFR _{CT}	64-slice DSCT Definition	On-site computation	≤ 0.80	13%
	CTA	128-slice DSCT Definition FLASH Siemens Healthcare	Siemens cFFR 1.4		
	TAG	Siemens Healthcare			
Zhang et al [43] <i>Plos One, 2016</i>	FFR _{CT}	64-slice Aquilion Toshiba	On-site computation	≤ 0.80	NA
	CTA	320-row CT Aquilion One Toshiba Medical Systems			
De Geer et al [44] <i>Acta Radiol, 2016</i>	FFR _{CT}	128-slice DSCT Definition FLASH Siemens Healthcare	On-site computation	≤ 0.80	NA
	CTA	128-slice DSCT Definition FLASH Siemens Healthcare	Siemens cFFR 1.4/1.7		
Kruk et al [45] <i>JACC Img, 2016</i>	FFR _{CT}	128-slice DSCT Definition FLASH Siemens Healthcare	On-site computation	≤ 0.80	6%
	CTA	Siemens Healthcare	Siemens cFFR 1.4		
Kawaji et al [46] <i>Int J Cardiovasc Img, 2016</i>	FFR _{CT}	64-slice DSCT Definition, Siemens	External laboratory	≤ 0.80	11%
	CTA	320-row CT Aquilion One Toshiba Medical Systems	Heart Flow 1.4		
Tesche et al [47] <i>JCCT, 2016</i>	FFR _{CT}	128-slice DSCT Definition FLASH Siemens Healthcare	On-site computation	≤ 0.80	6%
	TAG	Siemens Healthcare	Siemens cFFR 1.4		
Yang et al [30] <i>Eur heart J CV Img, 2017</i>	FFR _{CT}	128-slice DSCT Definition FLASH Siemens Healthcare	On-site computation	≤ 0.80	10%
	CTA	Siemens Healthcare	Siemens cFFR 1.4		
	CTP	Siemens Healthcare			
Coenen et al [31] <i>JACC Img, 2017</i>	FFR _{CT}	128-slice Definition FLASH, Siemens Healthcare	On-site computation	≤ 0.80	10%
	CTA	128-slice Definition FORCE Siemens Healthcare	Siemens cFFR 1.4		
	CTP	Siemens Healthcare			
Kurata et al [48] <i>Eur Radiol, 2017</i>	FFR _{CT}	128-slice DSCT Definition FLASH Siemens Healthcare	On-site computation	≤ 0.80	25%
	CTA	Siemens Healthcare	Siemens cFFR 1.4		
Osawa et al [49] <i>Heart vessels 2017</i>	FFR _{CT}	128-slice DSCT Definition FLASH Siemens Healthcare	External laboratory	≤ 0.80	10%
	CTA	Siemens Healthcare	Heart Flow 1.4		
Shi et al [50] <i>Biomed Eng Online, 2017</i>	FFR _{CT}	320-row CT Aquilion One Toshiba Medical Systems	On-site computation	≤ 0.80	NA
	CTA	Toshiba Medical Systems			
Ko et al [51] <i>JACC Img, 2017</i>	FFR _{CT}	320-row CT Aquilion One Toshiba Medical Systems	On-site computation	≤ 0.80	3%
	CTA	Toshiba Medical Systems	Toshiba		



Fig. 2 Quality assessment of included studies by QUADAS-2 Revised Criteria. QUADAS = Quality assessment of Diagnostic Accuracy Studies. Stacked bars represent the proportion of studies

with a low risk of bias, unclear risk of bias, or high risk of bias with regard to patient selection, utilized reference standard, and imaging modality (index test)

Table 4 Overall diagnostic accuracy on per-patient and per-vessel analysis

Index test	Studies	No. P or V	Sensitivity (95% CI)	Specificity (95% CI)	PPV (95% CI)	NPV (95% CI)	PLR (95% CI)	NLR (95% CI)	DOR (95% CI)	AUC (SE)	Q* (SE)
Patient level											
CTA	15	1537	0.91 (0.89–0.93)	0.48 (0.44–0.51)	0.59 (0.56–0.62)	0.87 (0.83–0.90)	1.78 (1.49–2.11)	0.20 (0.13–0.30)	10.58 (6.30–17.78)	0.80 (0.05)	0.74 (0.04)
Stress CTP	9	579	0.92 (0.88–0.95)	0.82 (0.76–0.86)	0.86 (0.82–0.90)	0.89 (0.84–0.93)	4.58 (3.54–5.91)	0.11 (0.08–0.17)	54.53 (30.47–97.56)	0.93 (0.02)	0.86 (0.02)
FFR _{CT}	8	823	0.88 (0.84–0.91)	0.72 (0.68–0.76)	0.70 (0.66–0.75)	0.90 (0.87–0.93)	3.45 (2.38–5.00)	0.18 (0.13–0.26)	19.79 (10.97–35.69)	0.90 (0.04)	0.83 (0.04)
Vessel level											
CTA	37	5351	0.86 (0.85–0.88)	0.64 (0.63–0.66)	0.53 (0.51–0.55)	0.91 (0.90–0.92)	2.42 (1.93–3.02)	0.21 (0.16–0.28)	12.32 (8.81–17.21)	0.82 (0.02)	0.75 (0.02)
Stress CTP	16	2336	0.82 (0.85–0.88)	0.89 (0.87–0.90)	0.79 (0.76–0.82)	0.91 (0.89–0.92)	7.72 (5.50–10.83)	0.21 (0.16–0.27)	50.77 (30.27–85.26)	0.94 (0.01)	0.88 (0.01)
FFR _{CT}	18	2071	0.85 (0.82–0.87)	0.75 (0.73–0.78)	0.65 (0.62–0.68)	0.90 (0.88–0.92)	3.50 (2.73–4.48)	0.23 (0.19–0.28)	18.11 (11.72–28.00)	0.89 (0.02)	0.82 (0.02)
TAG	10	930	0.57 (0.51–0.63)	0.62 (0.58–0.66)	0.41 (0.36–0.46)	0.76 (0.72–0.80)	1.97 (1.32–2.93)	0.67 (0.53–0.85)	3.20 (1.63–6.25)	0.65 (0.06)	0.61 (0.04)

P, patient; V, vessel; PPV, positive predictive value; NPV, negative predictive value; PLR, positive likelihood ratio; NLR, negative likelihood ratio; DOR, diagnostic odd ratio; AUC, area under the curve; CI, confidence interval; SE, standard error

vessels with or without hemodynamically significant CAD is influenced by cranio-caudal coverage.

Several prior meta-analyses assessed the diagnostic performance of different imaging techniques with iFFR as the reference standard, for the diagnosis of functionally significant CAD. In a previous published meta-analysis reporting 18 studies, Gonzalez et al reported similar diagnostic accuracy for CTA, CTP, and FFR_{CT}; however, they did not evaluate TAG [60]. Their results are similar to our analysis which indicated FFR_{CT} and CTP have higher PLR compared with CTA alone. Several other meta-analyses evaluated only FFR_{CT} as index test [61–67]. Their results are comparable to our findings, with AUC varying from 0.87 to 0.96 at per-patient level and 0.86 to 0.91 at per-vessel level. Takx et al analyzed diagnostic accuracy of different stress myocardial perfusion imaging techniques (SPECT, stress echo, positron emission tomography, MRI, and CTP) [68]. They evaluated seven stress CTP studies (three in dynamic and four in static mode) without separate analysis and reported global per-vessel PLR of 5.74 which is lower than our results (PLR of 7.72). In a separate analysis, we found lower performance for dynamic (PLR 4.8) than for static stress CTP (PLR 10.8). Danad et al evaluated diagnostic performance of multiple non-invasive methods (SPECT, stress echocardiography, invasive coronary angiography, CTA, FFR_{CT}, and MRI) [69]. For CTA (10 studies) and FFR_{CT} (3 studies), they reported quite similar results as those found in our study, with per-vessel PLR of 2.09 and 4.02 for CTA and FFR_{CT} respectively.

In our meta-analysis, we evaluate more recent studies (overall 50 studies) and focus on the comparison between all the cardiac-modalities including CTA alone, and all the different new emerging functional non-invasive methods such as stress CTP (16 studies), FFR_{CT} (18 studies), and TAG (10 studies).

Beyond diagnostic performance, other considerations are relevant to evaluate which test will be better to use in clinical practice, such as radiation exposure, contrast, availability, and costs [70–72]. From this point of view, stress CTP and FFR_{CT} have different strengths and shortcomings.

Stress CTP has the advantage of being a direct technique for myocardial ischemia assessment [73]. Myocardial CTP evaluation requires two scans: one with pharmacological stress and the other during rest. The rest acquisition is often used to coronary anatomy evaluation. Protocol can be performed according to the rest/stress or stress/rest sequences, separated by 10–20 min to allow for contrast wash-out: if the interval between the two acquisitions is too short, the residual contrast can cross contaminate the second scan. Hence, in the rest scan first approach, the contrast contamination of the myocardium during the second acquisition might mask an area of ischemia. In our meta-analysis, nine studies used rest phase first, and four studies stress phase first. For suitable clinical use, some authors proposed to use rest scan

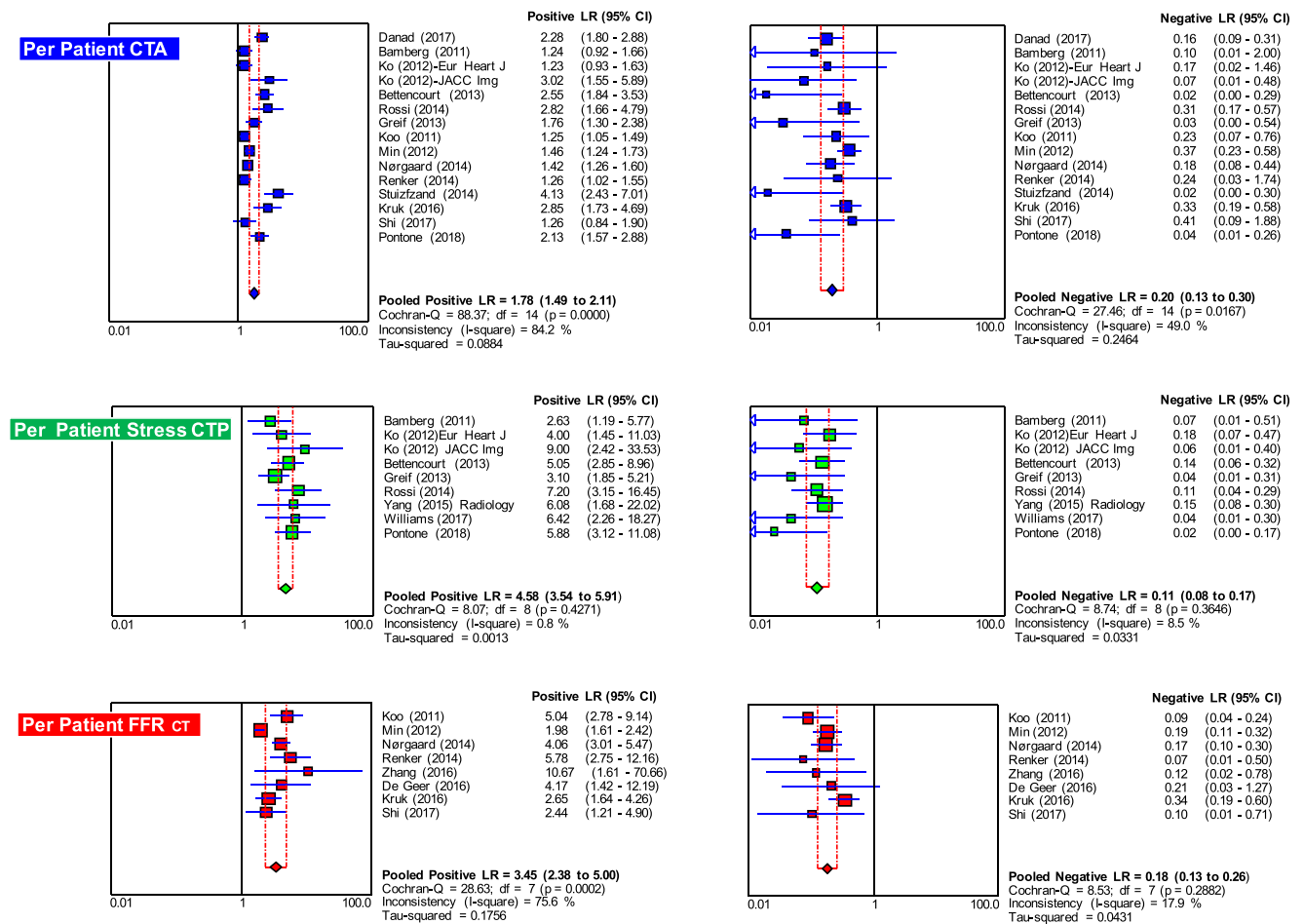


Fig. 3 Forest plots with pooled positive likelihood ratio and negative likelihood ratio across all the techniques for detection of hemodynamically significant coronary stenosis on a per-patient basis

compared to invasive FFR as a reference standard. CTA (blue dots); stress CTP (green dots); FFR_{CT} (red dots)

first for patients with lower pre-test probability of CAD, with the aim of ruling out CAD. Conversely, the stress scan first protocol, which has a better ability to detect ischemia, could be more appropriate for patients with high pre-test probability of CAD in whom there is a high clinical suspicion of significant functional CAD [74].

Stress acquisitions can be acquired using two different approaches: static or dynamic scans. Dynamic acquisition has the advantage of allowing quantitative assessment of myocardial perfusion while static only allows qualitative or semi-quantitative evaluation. Regardless of the acquisition protocol used, stress CTP requires the administration of a pharmacological stress agent and so double exposure to contrast agent and radiation. Another shortcoming of CTP is technical issue such as beam hardening artifacts. In the future, dual-energy CT techniques might reduce these artifacts. In this meta-analysis, none studies used dual-energy CT mode; but in an ongoing multi-centric study (Decide Gold), stress CTP will be performed using dual-energy technique and will evaluate potential reduction of beam hardening artifacts, by using virtual single-energy monochromatic imaging [75].

The FFR_{CT} is an indirect technique for functional assessment of CAD using coronary flow assessment to stress CTP, one of the main strength is that FFR_{CT} requires only one acquisition as it is quantified from standard CTA datasets, without modified protocol. Hence, this technique does not require stress agent, additional contrast, nor additional radiation. Another advantage over stress CTP is that FFR_{CT} has the ability to identify a specific coronary lesion that causes ischemia and open the way to a treatment strategy at a coronary artery lesion-specific level [71, 72]. However, FFR_{CT} is also associated with some limits: the first is the dependence on very high image quality. In our meta-analysis, even if studies were performed in experience cardiac imaging centers, a significant percentage of patients (from 3 up to 25%, when information was available) were excluded due to insufficient image quality. Furthermore, as pointed out by Cook et al, the diagnostic accuracy of FFR_{CT} varies substantially according to the spectrum of CAD (with high values at extremes of disease severity and lower values in the intermediate forms of disease) [66]. Finally, other limitations are software availability (most

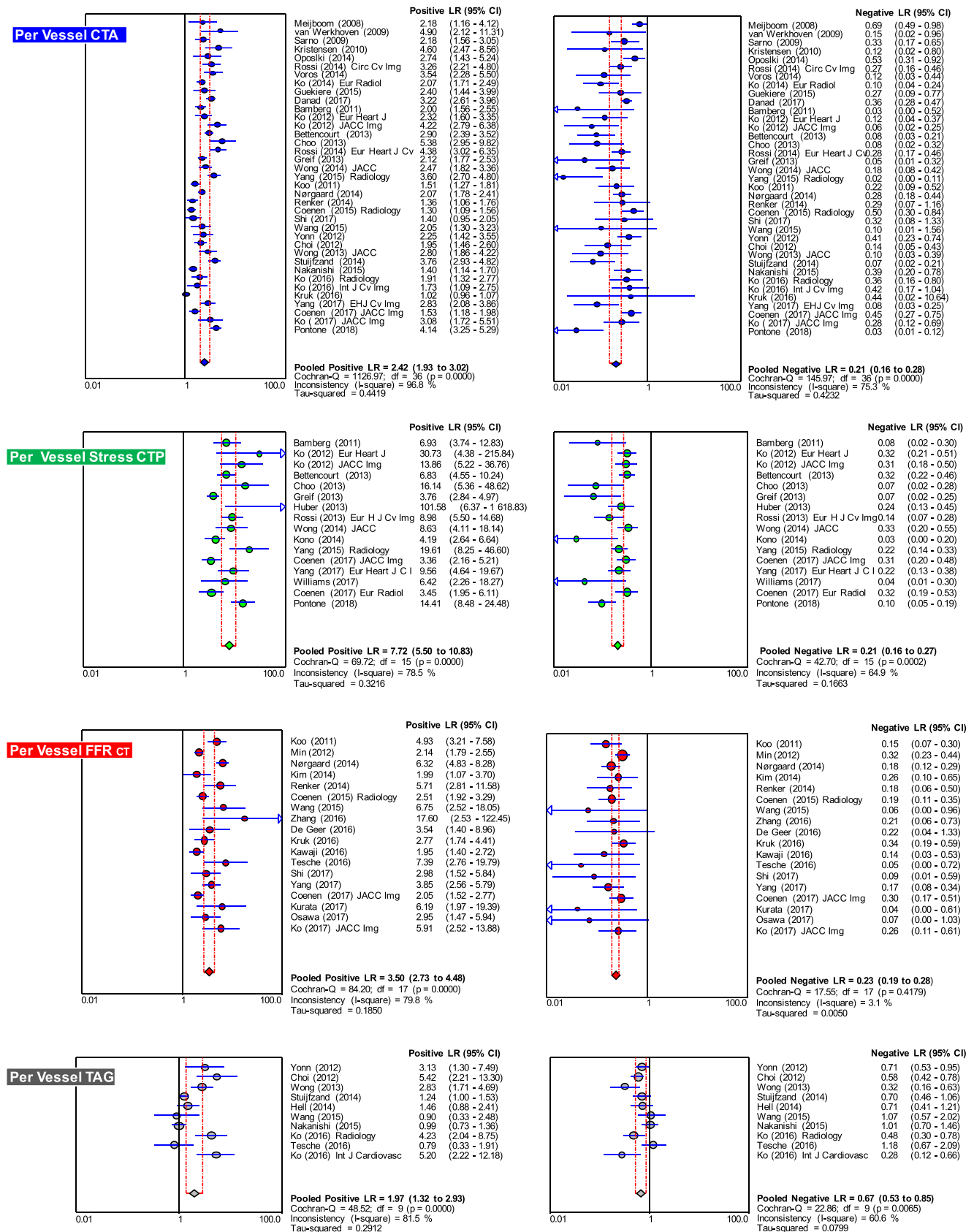
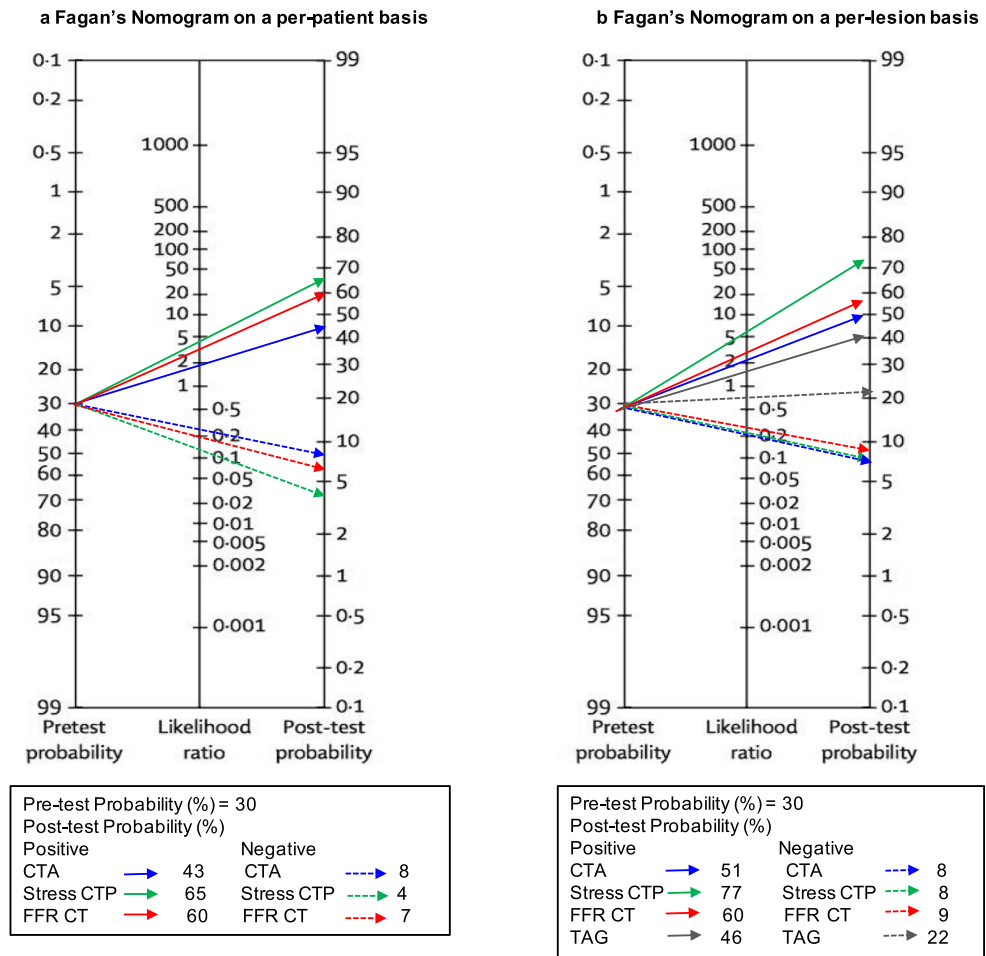


Fig. 4 Forest plots with pooled positive likelihood ration and negative likelihood ratio across all the techniques for detection of hemodynamically significant coronary stenosis on a per lesion basis compared to invasive FFR as a reference standard. CTA (blue dots); stress CTP (green dots); FFR_{CT} (red dots); TAG (gray dots)

Fig. 5 Fagan’s Nomogram plot analysis to evaluate the clinical utility of cardiac CT modalities for the detection of significant hemodynamically CAD using FFR as reference standard



multi-centric studies used off-site software analysis [36–39]), cost, and long post-processing time.

Our review highlights the need for further studies. By now, only one study, comprising a moderate number of patients, directly compared stress CTP and FFR_{CT}. They found comparable accuracy for the two techniques [31]. In our analysis, we found improved pooled specificity and PLR for stress CTP compared to FFR_{CT}. This difference points out that large prospective multicenter studies are warranted to determine if one of these technique yields better clinical utility. In the near future, PERFECTION prospective study (comparison between stress cardiac computed tomography PERfusion versus fractional flow rEserve measured by computed tomography angiography in the evaluation of suspected cOroNary artery disease) will directly prospectively evaluate the diagnostic accuracy of these two modalities [76]. Moreover, it will be interesting to evaluate the performance of these new CT modalities, in some classical real world situations such as in case of case of coronary artery stents, CABG, and coronary calcifications.

Among potential limitations of our meta-analysis, we can mention the different iFFR cutoff values used in the

included studies to define hemodynamically significant lesions. Moreover, different techniques for each modality have been combined in this analysis: included studies used various CT technology (64-slice to 320-slice CT), different acquisition protocols, different software for FFR_{CT}, different stress CTP post-processing, different methods, and cutoff for calculating TAG. The observed heterogeneity in the meta-analysis may have derived from those differences in imaging technology. Given this heterogeneity and small publication bias, our conclusions should be interpreted with caution. Furthermore, the external validity can be affected by expert center bias as most studies were performed at experienced imaging centers. Finally, most studies excluded patients with stents, coronary artery bypass grafts, chronic total occlusion and/or prior myocardial infarction and no conclusion can be given for these groups of patients.

Conclusion

In this meta-analysis comparing cardiac CT-based modalities directly to iFFR, stress CTP and FFR_{CT} have incremental

Table 5 Per-vessel sub-analysis for stress CTP, FFR_{CT}, and TAG

Index test	Studies	No. V	Sensitivity (95% CI)	Specificity (95% CI)	PPV (95% CI)	NPV (95% CI)	PLR (95% CI)	NLR (95% CI)	DOR (95% CI)	AUC (SE)	Q* (SE)
Vessel level											
Stress CTP	9	1398	0.80 (0.76–0.83)	0.93 (0.91–0.94)	0.85 (0.81–0.88)	0.90 (0.88–0.92)	10.77 (7.86–14.77)	0.23 (0.16–0.31)	59.04 (32.53–107.16)	0.96(0.01)	0.90 (0.02)
<i>Static mode</i>											
Stress CTP	7	938	0.85 (0.81–0.89)	0.83 (0.80–0.86)	0.72 (0.67–0.77)	0.92 (0.89–0.94)	4.89 (3.40–7.04)	0.17 (0.09–0.29)	42.45 (16.73–107.76)	0.94 (0.02)	0.87 (0.02)
<i>Dynamic mode</i>											
FFR _{CT}	6	1194	0.84 (0.80–0.88)	0.76 (0.73–0.79)	0.62 (0.58–0.66)	0.91 (0.89–0.93)	3.05 (1.89–4.93)	0.22 (0.15–0.31)	16.78 (7.24–38.88)	0.89 (0.03)	0.83 (0.04)
<i>Off-site analysis</i>											
FFR _{CT}	12	877	0.86 (0.81–0.89)	0.75 (0.71–0.79)	0.69 (0.64–0.73)	0.89 (0.86–0.92)	3.67 (2.79–4.82)	0.23 (0.18–0.29)	17.81 (10.81–29.33)	0.89 (0.02)	0.82 (0.02)
<i>On-site analysis</i>											
TAG	3	211	0.70 (0.58–0.80)	0.81 (0.74–0.87)	0.64 (0.54–0.76)	0.84 (0.77–0.90)	3.53 (2.43–5.13)	0.39 (0.27–0.56)	10.35 (5.26–20.38)	0.83 (0.04)	0.76 (0.04)
<i>320-slice CT</i>											
TAG	6	573	0.53 (0.45–0.61)	0.60 (0.55–0.64)	0.36 (0.30–0.42)	0.75 (0.70–0.80)	0.61 (1.00–2.60)	0.73 (0.60–0.88)	2.28 (1.13–4.61)	0.60 (0.05)	0.57 (0.04)
<i>< 320-slice CT</i>											

V, vessel; PPV, positive predictive value; NPV, negative predictive value; PLR, positive likelihood ratio; NLR, negative likelihood ratio; DOR, diagnostic odd ratio; AUC, area under the curve; CI, confidence interval; SE, standard error

value over CTA for non-invasive diagnosis of ischemia-causing CAD, with improved PLR and specificity in comparison to CTA alone.

Funding The authors state that this work has not received any funding.

Compliance with ethical standards

Guarantor The scientific guarantor of this publication is Dr. Michele Hamon (M.D.).

Conflict of interest The authors of this manuscript declare no relationships with any companies whose products or services may be related to the subject matter of the article.

Statistics and biometry One of the authors has significant statistical expertise.

Informed consent Written informed consent was not required for this study because it is a meta-analysis.

Ethical approval Institutional Review Board approval was not required because it is a meta-analysis.

Methodology

- Meta-analysis

References

- Hamon M, Biondi-Zoccai GG, Malagutti P et al (2006) Diagnostic performance of multislice spiral computed tomography of coronary arteries as compared with conventional invasive coronary angiography: a meta-analysis. *J Am Coll Cardiol* 48:1896–1910
- Montalescot G, Sechtem U, Achenbach S et al (2013) ESC guidelines on the management of stable coronary artery disease: the task force on the management of stable coronary artery disease of the European Society of Cardiology. *Eur Heart J* 34:2949–3003
- Gonçalves Pde A, Rodríguez-Granillo GA, Spitzer E et al (2015) Functional evaluation of coronary disease by CT angiography. *JACC Cardiovasc Imaging* 11:1322–1335
- Tonino PA, De Bruyne B, Pijls NH et al (2009) Fractional flow reserve versus angiography for guiding percutaneous coronary intervention. *N Engl J Med* 360:213–224
- De Bruyne B, Pijls NH, Kalesan B et al (2012) Fractional flow reserve-guided PCI versus medical therapy in stable coronary disease. *N Engl J Med* 367:991–1001
- Boden WE, O'Rourke RA, Teo KK et al (2007) Optimal medical therapy with or without PCI for stable coronary disease. *N Engl J Med* 356(15):1503–1516
- Liberati A, Altman DG, Tetzlaff J et al (2009) The PRISMA statement for reporting systematic reviews and meta-analyses of studies that evaluate healthcare interventions: explanation and elaboration. *BMJ* 339:b2700
- Whiting PF, Rutjes AW, Westwood ME et al (2011) QUADAS-2: a revised tool for the quality assessment of diagnostic accuracy studies. *Ann Intern Med* 8:529–536
- Zamora J, Abraira V, Muriel A, Khan K, Coomarasamy A (2006) Meta-DiSc: a software for meta-analysis of test accuracy data. *BMC Med Res Methodol* 6:31
- Meijboom WB, Van Mieghem CA, van Pelt N et al (2008) Comprehensive assessment of coronary artery stenoses: computed

- tomography coronary angiography versus conventional coronary angiography and correlation with fractional flow reserve in patients with stable angina. *J Am Coll Cardiol* 52:636–643
11. van Werkhoven JM, Schuijf JD, Jukema JW et al (2009) Comparison of non-invasive multi-slice computed tomography coronary angiography versus invasive coronary angiography and fractional flow reserve for the evaluation of men with known coronary artery disease. *Am J Cardiol* 104:653–656
 12. Sarno G, Decraemer I, Vanhoenacker PK et al (2009) On the inappropriateness of noninvasive multidetector computed tomography coronary angiography to trigger coronary revascularization: a comparison with invasive angiography. *JACC Cardiovasc Interv* 2:550–557
 13. Kristensen TS, Engstrøm T, Kelbæk H, von der Recke P, Nielsen MB, Kofoed KF (2010) Correlation between coronary computed tomographic angiography and fractional flow reserve. *Int J Cardiol* 144:200–205
 14. Opolski MP, Kepka C, Achenbach S et al (2014) Advanced computed tomographic anatomical and morphometric plaque analysis for prediction of fractional flow reserve in intermediate coronary lesions. *Eur J Radiol* 83:135–141
 15. Rossi A, Papadopoulou SL, Pugliese F et al (2014) Quantitative computed tomographic coronary angiography: does it predict functionally significant coronary stenoses? *Circ Cardiovasc Imaging* 1:43–51
 16. Voros S, Rinehart S, Vazquez-Figueroa JG et al (2014) Prospective, head-to-head comparison of quantitative coronary angiography, quantitative computed tomography angiography, and intravascular ultrasound for the prediction of hemodynamic significance in intermediate and severe lesions, using fractional flow reserve as reference standard (from the ATLANTA I and II Study). *Am J Cardiol* 113:23–29
 17. Ko BS, Wong DT, Cameron JD et al (2014) 320-row CT coronary angiography predicts freedom from revascularisation and acts as a gatekeeper to defer invasive angiography in stable coronary artery disease: a fractional flow reserve-correlated study. *Eur Radiol* 24:738–747
 18. Ghekiere O, Dewilde W, Bellekens M et al (2015) Diagnostic performance of quantitative coronary computed tomography angiography and quantitative coronary angiography to predict hemodynamic significance of intermediate-grade stenoses. *Int J Cardiovasc Imaging* 31:1651–1661
 19. Danad I, Rajmakers PG, Driessen R et al (2017) Comparison of coronary angiography, SPECT, PET, and hybrid imaging for diagnosis of ischemic heart disease determined by fractional flow reserve. *JAMA Cardiol* 2(10):1100–1107
 20. Bamberg F, Becker A, Schwarz F et al (2011) Detection of hemodynamically significant coronary artery stenosis: incremental diagnostic value of dynamic CT-based myocardial perfusion imaging. *Radiology* 260:689–698
 21. Ko BS, Cameron JD, Meredith IT et al (2012) Computed tomography stress myocardial perfusion imaging in patients considered for revascularization: a comparison with fractional flow reserve. *Eur Heart J* 33:67–77
 22. Ko BS, Cameron JD, Leung M et al (2012) Combined CT coronary angiography and stress myocardial perfusion imaging for hemodynamically significant stenoses in patients with suspected coronary artery disease: a comparison with fractional flow reserve. *JACC Cardiovasc Imaging* 5:1097–1111
 23. Bettencourt N, Chiribiri A, Schuster A et al (2013) Direct comparison of cardiac magnetic resonance and multidetector computed tomography stress-rest perfusion imaging for detection of coronary artery disease. *J Am Coll Cardiol* 61:1099–1107
 24. Choo KS, Hwangbo L, Kim JH et al (2013) Adenosine-stress low-dose single-scan CT myocardial perfusion imaging using a 128-slice dual-source CT: a comparison with fractional flow reserve. *Acta Radiol* 54:389–395
 25. Greif M, von Ziegler F, Bamberg F et al (2013) CT stress perfusion imaging for detection of haemodynamically relevant coronary stenosis as defined by FFR. *Heart* 99:1004–1111
 26. Huber AM, Leber V, Gramer BM et al (2013) Myocardium: dynamic versus single-shot CT perfusion imaging. *Radiology* 269:378–386
 27. Rossi A, Dharampal A, Wragg A et al (2014) Diagnostic performance of hyperaemic myocardial blood flow index obtained by dynamic computed tomography: does it predict functionally significant coronary lesions? *Eur Heart J Cardiovasc Imaging* 15:85–94
 28. Wong DT, Ko BS, Cameron JD et al (2014) Comparison of diagnostic accuracy of combined assessment using adenosine stress computed tomography perfusion + computed tomography angiography with transluminal attenuation gradient + computed tomography angiography against invasive fractional flow reserve. *J Am Coll Cardiol* 63:1904–1912
 29. Kono AK, Coenen A, Lubbers MM et al (2014) Relative myocardial blood flow by dynamic computed tomographic perfusion imaging predicts hemodynamic significance of coronary stenosis better than absolute blood flow. *Invest Radiol* 49:801–807
 30. Yang DH, Kim YH, Roh JH et al (2015) Stress myocardial perfusion CT in patients suspected of having coronary artery disease: visual and quantitative analysis-validation by using fractional flow reserve. *Radiology* 276:715–723
 31. Coenen A, Rossi A, Lubbers MM et al (2017) Integrating CT myocardial perfusion and CT-FFR in the work-up of coronary artery disease. *JACC Cardiovasc Imaging* 10:760–770
 32. Yang DH, Kim YH, Roh JH et al (2017) Diagnostic performance of on-site CT-derived fractional flow reserve versus CT perfusion. *Eur Heart J Cardiovasc Imaging* 18:432–440
 33. Williams MC, Mirsadraee S, Dweck MR et al (2017) Computed tomography myocardial perfusion vs ¹⁵O-water positron emission tomography and fractional flow reserve. *Eur Radiol* 27:1114–1124
 34. Coenen A, Lubbers MM, Kurata A et al (2017) Diagnostic value of transmural perfusion ratio derived from dynamic CT-based myocardial perfusion imaging for the detection of haemodynamically relevant coronary artery stenosis. *Eur Radiol* 27:2309–2316
 35. Pontone G, Andreini D, Guaricci AI et al (2018) Incremental diagnostic value of stress computed tomography myocardial perfusion with whole-heart coverage CT scanner in intermediate- to high risk symptomatic patients suspected of coronary artery disease. *JACC Cardiovasc Imaging*. Available online 14 February 2018. <https://doi.org/10.1016/j.jcmg.2017.10.025>
 36. Koo BK, Erglis A, Doh JH et al (2011) Diagnosis of ischemia-causing coronary stenoses by noninvasive fractional flow reserve computed from coronary computed tomographic angiograms. Results from the prospective multicenter DISCOVER-FLOW (Diagnosis of Ischemia-Causing Stenoses Obtained Via Noninvasive Fractional Flow Reserve) study. *J Am Coll Cardiol* 58:1989–1997
 37. Min JK, Leipsic J, Pencina MJ et al (2012) Diagnostic accuracy of fractional flow reserve from anatomic CT angiography. *JAMA* 308:1237–1245
 38. Nørgaard BL, Leipsic J, Gaur S et al (2014) Diagnostic performance of noninvasive fractional flow reserve derived from coronary computed tomography angiography in suspected coronary artery disease: the NXT trial (Analysis of Coronary Blood Flow Using CT Angiography: Next Steps). *J Am Coll Cardiol* 63:1145–1155
 39. Kim KH, Doh JH, Koo BK et al (2014) A novel noninvasive technology for treatment planning using virtual coronary stenting and computed tomography-derived computed fractional flow reserve. *JACC Cardiovasc Interv* 7:72–78
 40. Renker M, Schoepf UJ, Wang R et al (2014) Comparison of diagnostic value of a novel noninvasive coronary computed tomography angiography method versus standard coronary angiography for assessing fractional flow reserve. *Am J Cardiol* 114:1303–1308

41. Coenen A, Lubbers MM, Kurata A et al (2015) Fractional flow reserve computed from noninvasive CT angiography data: diagnostic performance of an on-site clinician-operated computational fluid dynamics algorithm. *Radiology* 274:674–683
42. Wang R, Renker M, Schoepf UJ et al (2015) Diagnostic value of quantitative stenosis predictors with coronary CT angiography compared to invasive fractional flow reserve. *Eur J Radiol* 84:1509–1515
43. Zhang JM, Zhong L, Luo T et al (2016) Simplified models of non-invasive fractional flow reserve based on CT images. *PLoS One* 11(5):e0153070
44. De Geer J, Sandstedt M, Björkholm A et al (2016) Software-based on-site estimation of fractional flow reserve using standard coronary CT angiography data. *Acta Radiol* 57:1186–1192
45. Kruk M, Wardziak L, Demkov M et al (2016) Workstation-based calculation of CTA-based FFR for intermediate stenosis. *JACC Cardiovasc Imaging* 9:690–699
46. Kawaji T, Shiomi H, Morishita H et al (2017) Feasibility and diagnostic performance of fractional flow reserve measurement derived from coronary computed tomography angiography in real clinical practice. *Int J Cardiovasc Imaging* 33:271–281
47. Tesche C, De Cecco CN, Caruso D et al (2017) Coronary CT angiography derived morphological and functional quantitative plaque markers correlated with invasive fractional flow reserve for detecting hemodynamically significant stenosis. *J Cardiovasc Comput Tomogr* 10:199–206
48. Kurata A, Coenen A, Lubbers MM et al (2017) The effect of blood pressure on non-invasive fractional flow reserve derived from coronary computed tomography angiography. *Eur Radiol* 27:1416–1423
49. Osawa K, Miyoshi T, Miki T et al (2017) Coronary lesion characteristics with mismatch between fractional flow reserve derived from CT and invasive catheterization in clinical practice. *Heart Vessels* 32:390–398
50. Shi C, Zhang D, Cao K et al (2017) A study of noninvasive fractional flow reserve derived from a simplified method based on coronary computed tomography angiography in suspected coronary artery disease. *Biomed Eng Online*. <https://doi.org/10.1186/s12938-017-0330-2>
51. Ko BS, Cameron JD, Munnur RK et al (2017) Noninvasive CT-derived FFR based on structural and fluid analysis. A comparison with invasive FFR for detection of functionally significant stenosis. *JACC Cardiovasc Imaging* 10:663–673
52. Yoon YE, Choi JH, Kim JH et al (2012) Noninvasive diagnosis of ischaemia-causing coronary stenosis using CT angiography: diagnostic value of transluminal attenuation gradient and fractional flow reserve computed from coronary CT angiography compared to invasively measured fractional flow reserve. *JACC Cardiovasc Imaging* 5:1088–1016
53. Choi JH, Koo BK, Yoon YE et al (2012) Diagnostic performance of intracoronary gradient-based methods by coronary computed tomography angiography for the evaluation of physiologically significant coronary artery stenoses: a validation study with fractional flow reserve. *Eur Heart J Cardiovasc Imaging* 13:1001–1007
54. Wong DT, Ko BS, Cameron JD et al (2013) Transluminal attenuation gradient in coronary computed tomography angiography is a novel noninvasive approach to the identification of functionally significant coronary artery stenosis: a comparison with fractional flow reserve. *J Am Coll Cardiol* 61:1271–1279
55. Stuijzfand WJ, Danad I, Raijmakers PG et al (2014) Additional value of transluminal attenuation gradient in CT angiography to predict hemodynamic significance of coronary artery stenosis. *JACC Cardiovasc Imaging* 7:374–386
56. Hell MM, Dey D, Marwan M, Achenbach S, Schmid J, Schuhbaeck A (2015) Non-invasive prediction of hemodynamically significant coronary artery stenoses by contrast density difference in coronary CT angiography. *Eur J Radiol* 84:1502–1508
57. Nakanishi R, Matsumoto S, Alani A et al (2015) Diagnostic performance of transluminal attenuation gradient and fractional flow reserve by coronary computed tomographic angiography (FFR(CT)) compared to invasive FFR: a sub-group analysis from the DISCOVER-FLOW and DeFACTO studies. *Int J Cardiovasc Imaging* 31:1251–1259
58. Ko BS, Wong DT, Nørgaard BL et al (2016) Diagnostic performance of transluminal attenuation gradient and noninvasive fractional flow reserve derived from 320-detector row CT angiography to diagnose hemodynamically significant coronary stenosis: an NXT substudy. *Radiology* 279:75–83
59. Ko BS, Seneviratne S, Cameron J et al (2016) Rest and stress transluminal attenuation gradient and contrast opacification difference for detection of hemodynamically significant stenosis in patients with suspected coronary artery disease. *Int J Cardiovasc Imaging* 32:1131–1141
60. Gonzalez JA, Lipinski MJ, Flors L, Shaw PW, Kramer CM, Salerno M (2015) Meta-analysis of diagnostic performance of computed tomography, computed tomography perfusion and computed-tomography- fractional flow reserve in functional myocardial ischemia assessment versus invasive fractional flow reserve. *Am J Cardiol* 116:1469–1478
61. Xu R, Li C, Qian J, Ge J (2015) Computed tomography-derived fractional flow reserve in the detection of lesion-specific ischemia. *Medicine (Baltimore)* 94(46):e1963
62. Deng S, Jing XD, Wang J et al (2015) Diagnostic performance of noninvasive fractional flow reserve derived from coronary computed tomography angiography in coronary artery disease: a systematic review and meta-analysis. *Int J Cardiol* 184:703–709
63. Li S, Tang X, Peng L, Luo Y, Dong R, Liu J (2015) The diagnostic performance of CT-derived fractional flow reserve for evaluation of myocardial ischemia confirmed by invasive fractional flow reserve: a meta-analysis. *Clin Radiol* 70:476–486
64. Ding A, Qiu G, Lin W et al (2016) Diagnostic performance of noninvasive fractional flow reserve derived from coronary computed tomography angiography in ischaemia-causing coronary stenosis: a meta-analysis. *Jpn J Radiol* 34:795808
65. Wu W, Pan DR, Foin N et al (2016) Noninvasive fractional flow reserve derived from coronary computed tomography angiography for identification of ischemic lesions: a systematic review and meta-analysis. *Sci Rep* 6:29409
66. Cook CM, Petraco R, Shun-Shin M et al (2017) Diagnostic accuracy of computed tomography-derived fractional flow reserve. A systematic review. *JAMA Cardiol* 2:803–810
67. Baumann S, Renker M, Hetjens S et al (2016) Comparison of coronary computed tomography angiography-derived vs invasive fractional flow reserve assessment: meta-analysis with subgroup of intermediate stenosis. *Acad Radiol* 23:1402–1411
68. Takx RA, Blomberg BA, El Aidi H et al (2015) Diagnostic accuracy of stress myocardial perfusion imaging compared to invasive coronary angiography with fractional flow reserve meta-analysis. *Circ Cardiovasc Imaging* 8:e002666
69. Danad I, Szymonifka J, Twisk JW et al (2017) Diagnostic performance of cardiac imaging methods to diagnose ischaemia-causing coronary artery disease when directly compared with fractional flow reserve as a reference standard: a meta-analysis. *Eur Heart J* 38:991–998
70. Xu L, Sun Z, Fan Z (2015) Noninvasive physiologic assessment of coronary stenoses using cardiac CT. *Biomed Res Int* 2015:435737
71. Cademartiri F, Seitun S, Clemente A et al (2017) Myocardial blood flow quantification for evaluation of coronary artery disease by computed tomography. *Cardiovasc Diagn Ther* 7:129–150
72. Pontone G, Muscogiuri G, Andreini D et al (2016) The new frontier of cardiac computed tomography angiography: fractional flow reserve and stress myocardial perfusion. *Curr Treat Options Cardiovasc Med* 18:74

73. Rossi A, Merkus D, Klotz E, Mollet N, de Feyter PJ, Krestin GP (2014) Stress myocardial perfusion: imaging with multidetector CT. *Radiology* 270:25–46
74. Tehasith T, Cury RC (2011) Stress Myocardial CT perfusion: an update and future perspective. *JACC Cardiovasc Imaging* 4: 905–916
75. Truong QA, Knaapen P, Pontone G et al (2015) Rationale and design of the dual-energy computed tomography for ischemia determination compared to “gold standard” non-invasive and invasive techniques (DECIDE-gold): a multicenter international efficacy diagnostic study of rest-stress dual-energy computed tomography angiography with perfusion. *J Nucl Cardiol* 22:1031–1040
76. Pontone G, Andreini D, Guaricci AI et al (2016) Rationale and design of the PERFECTION (comparison between stress cardiac computed tomography PERfusion versus fractional flow rEserve measured by computed tomography angiography in the evaluation of suspected cOroNary artery disease) prospective study. *J Cardiovasc Comput Tomogr* 10:330–334